

MOVEGPT: SCALING MOBILITY FOUNDATION MODELS WITH SPATIALLY-AWARE MIXTURE OF EXPERTS

000
001
002
003
004
005 **Anonymous authors**
006 Paper under double-blind review
007
008
009
010
011
012
013
014
015
016
017
018
019
020
021
022
023
024
025
026
027
028
029
030
031
032
033
034
035
036
037
038
039
040
041
042
043
044
045
046
047
048
049
050
051
052
053
054
055
056
057
058
059
060
061
062
063
064
065
066
067
068
069
070
071
072
073
074
075
076
077
078
079
080
081
082
083
084
085
086
087
088
089
090
091
092
093
094
095
096
097
098
099
100
101
102
103
104
105
106
107
108
109
110
111
112
113
114
115
116
117
118
119
120
121
122
123
124
125
126
127
128
129
130
131
132
133
134
135
136
137
138
139
140
141
142
143
144
145
146
147
148
149
150
151
152
153
154
155
156
157
158
159
160
161
162
163
164
165
166
167
168
169
170
171
172
173
174
175
176
177
178
179
180
181
182
183
184
185
186
187
188
189
190
191
192
193
194
195
196
197
198
199
200
201
202
203
204
205
206
207
208
209
210
211
212
213
214
215
216
217
218
219
220
221
222
223
224
225
226
227
228
229
230
231
232
233
234
235
236
237
238
239
240
241
242
243
244
245
246
247
248
249
250
251
252
253
254
255
256
257
258
259
260
261
262
263
264
265
266
267
268
269
270
271
272
273
274
275
276
277
278
279
280
281
282
283
284
285
286
287
288
289
290
291
292
293
294
295
296
297
298
299
300
301
302
303
304
305
306
307
308
309
310
311
312
313
314
315
316
317
318
319
320
321
322
323
324
325
326
327
328
329
330
331
332
333
334
335
336
337
338
339
340
341
342
343
344
345
346
347
348
349
350
351
352
353
354
355
356
357
358
359
360
361
362
363
364
365
366
367
368
369
370
371
372
373
374
375
376
377
378
379
380
381
382
383
384
385
386
387
388
389
390
391
392
393
394
395
396
397
398
399
400
401
402
403
404
405
406
407
408
409
410
411
412
413
414
415
416
417
418
419
420
421
422
423
424
425
426
427
428
429
430
431
432
433
434
435
436
437
438
439
440
441
442
443
444
445
446
447
448
449
450
451
452
453
454
455
456
457
458
459
460
461
462
463
464
465
466
467
468
469
470
471
472
473
474
475
476
477
478
479
480
481
482
483
484
485
486
487
488
489
490
491
492
493
494
495
496
497
498
499
500
501
502
503
504
505
506
507
508
509
510
511
512
513
514
515
516
517
518
519
520
521
522
523
524
525
526
527
528
529
530
531
532
533
534
535
536
537
538
539
540
541
542
543
544
545
546
547
548
549
550
551
552
553
554
555
556
557
558
559
559
560
561
562
563
564
565
566
567
568
569
569
570
571
572
573
574
575
576
577
578
579
579
580
581
582
583
584
585
586
587
588
589
589
590
591
592
593
594
595
596
597
598
599
599
600
601
602
603
604
605
606
607
608
609
609
610
611
612
613
614
615
616
617
618
619
619
620
621
622
623
624
625
626
627
628
629
629
630
631
632
633
634
635
636
637
638
639
639
640
641
642
643
644
645
646
647
648
649
649
650
651
652
653
654
655
656
657
658
659
659
660
661
662
663
664
665
666
667
668
669
669
670
671
672
673
674
675
676
677
678
679
679
680
681
682
683
684
685
686
687
688
689
689
690
691
692
693
694
695
696
697
698
699
699
700
701
702
703
704
705
706
707
708
709
709
710
711
712
713
714
715
716
717
718
719
719
720
721
722
723
724
725
726
727
728
729
729
730
731
732
733
734
735
736
737
738
739
739
740
741
742
743
744
745
746
747
748
749
749
750
751
752
753
754
755
756
757
758
759
759
760
761
762
763
764
765
766
767
768
769
769
770
771
772
773
774
775
776
777
778
779
779
780
781
782
783
784
785
786
787
788
789
789
790
791
792
793
794
795
796
797
798
799
799
800
801
802
803
804
805
806
807
808
809
809
810
811
812
813
814
815
816
817
818
819
819
820
821
822
823
824
825
826
827
828
829
829
830
831
832
833
834
835
836
837
838
839
839
840
841
842
843
844
845
846
847
848
849
849
850
851
852
853
854
855
856
857
858
859
859
860
861
862
863
864
865
866
867
868
869
869
870
871
872
873
874
875
876
877
878
879
879
880
881
882
883
884
885
886
887
888
889
889
890
891
892
893
894
895
896
897
898
899
899
900
901
902
903
904
905
906
907
908
909
909
910
911
912
913
914
915
916
917
918
919
919
920
921
922
923
924
925
926
927
928
929
929
930
931
932
933
934
935
936
937
938
939
939
940
941
942
943
944
945
946
947
948
949
949
950
951
952
953
954
955
956
957
958
959
959
960
961
962
963
964
965
966
967
968
969
969
970
971
972
973
974
975
976
977
978
979
979
980
981
982
983
984
985
986
987
988
989
989
990
991
992
993
994
995
996
997
998
999
1000
1001
1002
1003
1004
1005
1006
1007
1008
1009
1009
1010
1011
1012
1013
1014
1015
1016
1017
1018
1019
1019
1020
1021
1022
1023
1024
1025
1026
1027
1028
1029
1029
1030
1031
1032
1033
1034
1035
1036
1037
1038
1039
1040
1041
1042
1043
1044
1045
1046
1047
1048
1049
1050
1051
1052
1053
1054
1055
1056
1057
1058
1059
1059
1060
1061
1062
1063
1064
1065
1066
1067
1068
1069
1069
1070
1071
1072
1073
1074
1075
1076
1077
1078
1079
1079
1080
1081
1082
1083
1084
1085
1086
1087
1088
1089
1089
1090
1091
1092
1093
1094
1095
1096
1097
1098
1099
1099
1100
1101
1102
1103
1104
1105
1106
1107
1108
1109
1109
1110
1111
1112
1113
1114
1115
1116
1117
1118
1119
1119
1120
1121
1122
1123
1124
1125
1126
1127
1128
1129
1129
1130
1131
1132
1133
1134
1135
1136
1137
1138
1139
1139
1140
1141
1142
1143
1144
1145
1146
1147
1148
1149
1149
1150
1151
1152
1153
1154
1155
1156
1157
1158
1159
1159
1160
1161
1162
1163
1164
1165
1166
1167
1168
1169
1169
1170
1171
1172
1173
1174
1175
1176
1177
1178
1179
1179
1180
1181
1182
1183
1184
1185
1186
1187
1188
1189
1189
1190
1191
1192
1193
1194
1195
1196
1197
1198
1199
1199
1200
1201
1202
1203
1204
1205
1206
1207
1208
1209
1209
1210
1211
1212
1213
1214
1215
1216
1217
1218
1219
1219
1220
1221
1222
1223
1224
1225
1226
1227
1228
1229
1229
1230
1231
1232
1233
1234
1235
1236
1237
1238
1239
1239
1240
1241
1242
1243
1244
1245
1246
1247
1248
1249
1249
1250
1251
1252
1253
1254
1255
1256
1257
1258
1259
1259
1260
1261
1262
1263
1264
1265
1266
1267
1268
1269
1269
1270
1271
1272
1273
1274
1275
1276
1277
1278
1279
1279
1280
1281
1282
1283
1284
1285
1286
1287
1288
1289
1289
1290
1291
1292
1293
1294
1295
1296
1297
1298
1299
1299
1300
1301
1302
1303
1304
1305
1306
1307
1308
1309
1309
1310
1311
1312
1313
1314
1315
1316
1317
1318
1319
1319
1320
1321
1322
1323
1324
1325
1326
1327
1328
1329
1329
1330
1331
1332
1333
1334
1335
1336
1337
1338
1339
1339
1340
1341
1342
1343
1344
1345
1346
1347
1348
1349
1349
1350
1351
1352
1353
1354
1355
1356
1357
1358
1359
1359
1360
1361
1362
1363
1364
1365
1366
1367
1368
1369
1369
1370
1371
1372
1373
1374
1375
1376
1377
1378
1379
1379
1380
1381
1382
1383
1384
1385
1386
1387
1388
1389
1389
1390
1391
1392
1393
1394
1395
1396
1397
1398
1399
1399
1400
1401
1402
1403
1404
1405
1406
1407
1408
1409
1409
1410
1411
1412
1413
1414
1415
1416
1417
1418
1419
1419
1420
1421
1422
1423
1424
1425
1426
1427
1428
1429
1429
1430
1431
1432
1433
1434
1435
1436
1437
1438
1439
1439
1440
1441
1442
1443
1444
1445
1446
1447
1448
1449
1449
1450
1451
1452
1453
1454
1455
1456
1457
1458
1459
1459
1460
1461
1462
1463
1464
1465
1466
1467
1468
1469
1469
1470
1471
1472
1473
1474
1475
1476
1477
1478
1479
1479
1480
1481
1482
1483
1484
1485
1486
1487
1488
1489
1489
1490
1491
1492
1493
1494
1495
1496
1497
1498
1499
1499
1500
1501
1502
1503
1504
1505
1506
1507
1508
1509
1509
1510
1511
1512
1513
1514
1515
1516
1517
1518
1519
1519
1520
1521
1522
1523
1524
1525
1526
1527
1528
1529
1529
1530
1531
1532
1533
1534
1535
1536
1537
1538
1539
1539
1540
1541
1542
1543
1544
1545
1546
1547
1548
1549
1549
1550
1551
1552
1553
1554
1555
1556
1557
1558
1559
1559
1560
1561
1562
1563
1564
1565
1566
1567
1568
1569
1569
1570
1571
1572
1573
1574
1575
1576
1577
1578
1579
1579
1580
1581
1582
1583
1584
1585
1586
1587
1588
1589
1589
1590
1591
1592
1593
1594
1595
1596
1597
1598
1599
1599
1600
1601
1602
1603
1604
1605
1606
1607
1608
1609
1609
1610
1611
1612
1613
1614
1615
1616
1617
1618
1619
1619
1620
1621
1622
1623
1624
1625
1626
1627
1628
1629
1629
1630
1631
1632
1633
1634
1635
1636
1637
1638
1639
1639
1640
1641
1642
1643
1644
1645
1646
1647
1648
1649
1649
1650
1651
1652
1653
1654
1655
1656
1657
1658
1659
1659
1660
1661
1662
1663
1664
1665
1666
1667
1668
1669
1669
1670
1671
1672
1673
1674
1675
1676
1677
1678
1679
1679
1680
1681
1682
1683
1684
1685
1686
1687
1688
1689
1689
1690
1691
1692
1693
1694
1695
1696
1697
1698
1699
1699
1700
1701
1702
1703
1704
1705
1706
1707
1708
1709
1709
1710
1711
1712
1713
1714
1715
1716
1717
1718
1719
1719
1720
1721
1722
1723
1724
1725
1726
1727
1728
1729
1729
1730
1731
1732
1733
1734
1735
1736
1737
1738
1739
1739
1740
1741
1742
1743
1744
1745
1746
1747
1748
1749
1749
1750
1751
1752
1753
1754
1755
1756
1757
1758
1759
1759
1760
1761
1762
1763
1764
1765
1766
1767
1768
1769
1769
1770
1771
1772
1773
1774
1775
1776
1777
1778
1779
1779
1780
1781
1782
1783
1784
1785
1786
1787
1788
1789
1789
1790
1791
1792
1793
1794
1795
1796
1797
1798
1799
1799
1800
1801
1802
1803
1804
1805
1806
1807
1808
1809
1809
1810
1811
1812
1813
1814
1815
1816
1817
1818
1819
1819
1820
1821
1822
1823
1824
1825
1826
1827
1828
1829
1829
1830
1831
1832
1833
1834
1835
1836
1837
1838
1839
1839
1840
1841
1842
1843
1844
1845
1846
1847
1848
1849
1849
1850
1851
1852
1853
1854
1855
1856
1857
1858
1859
1859
1860
1861
1862
1863
1864
1865
1866
1867
1868
1869
1869
1870
1871
1872
1873
1874
1875
1876
1877
1878
1879
1879
1880
1881
1882
1883
1884
1885
1886
1887
1888
1889
1889
1890
1891
1892
1893
1894
1895
1896
1897
1898
1899
1899
1900
1901
1902
1903
1904
1905
1906
1907
1908
1909
1909
1910
1911
1912
1913
1914<br

054
055 **Table 1: Comparison between existing models and MoveGPT across key aspects.**
056

Method	Model Init.	Unit	Temp. Regularity	Geo. Scalability	Task Flexibility	#Param
TrajFM (Lin et al., 2024)	Scratch	Raw GPS	Irregular	✓	✗	18M
UniTraj (zhu2024unitraj	Scratch	Raw GPS	Irregular	✓	✓	2.3M
TrajGPT (Hsu et al., 2024)	Scratch	Stay Point	Irregular	✗	✗	20w
TrajGDM (Chu et al., 2023)	Scratch	Stay Point	Irregular	✗	✗	28M
UniMove (Han et al., 2025)	Scratch	Stay Point	Irregular	✓	✗	40M
GenMove (Long et al., 2025a)	Scratch	Zone ID	Regular	✗	✗	21M
UniMob (Long et al., 2025b)	Scratch	Zone ID	Regular	✗	✓	6M
UniST (Yuan et al., 2024a)	Scratch	Zone ID	Regular	✓	✓	30M
UrbanGPT (Li et al., 2024b)	LLMs	Zone ID	Regular	✓	✗	-
UrbanDiT (Yuan et al., 2024b)	Scratch	Zone ID	Regular	✓	✓	30M
MoveGPT	Scratch	Stay Point	Irregular	✓	✓	261M

064
065 mobility (Song et al., 2010b; Schneider et al., 2013). This combination of massive data and intrinsic
066 predictability creates the ideal conditions to move beyond task-specific statistical models and towards
067 a more holistic and generalizable understanding Zhou et al. (2024).

068 Inspired by the transformative success of foundation models in language, a new wave of general-
069 purpose models for mobility has emerged, such as UniST Yuan et al. (2024a), UrbanDiT Yuan
070 et al. (2024b), TrajFM Lin et al. (2024), TrajGPT Hsu et al. (2024), UniMob Long et al. (2025b),
071 GenMove Long et al. (2025a), and UniTraj Zhu et al. (2024). However, these pioneering efforts,
072 while valuable, fall short of creating a true “GPT for mobility”. A detailed comparison, summarized
073 in Table 1, reveals several practical limitations shared by current approaches. Specifically, they rely
074 on inconsistent basic units to represent movement, from raw GPS coordinates to non-transferable
075 Zone IDs, a fragmentation that directly hinders their geographic scalability and prevents cross-city
076 pre-training. Furthermore, many of these models exhibit limited task flexibility and are constrained
077 in their parameter scale, which prevents them from fully leveraging the rich patterns within large,
078 diverse mobility datasets.
079

080 We argue these practical limitations stem from two fundamental yet unsolved barriers. The first barrier
081 is the lack of a universal basic unit, which directly prevents the scaling of data across geographies.
082 For instance, some models define tokens as aggregated spatio-temporal patches (e.g., UniST Yuan
083 et al. (2024a), UrbanDiT Yuan et al. (2024b)), an approach too coarse to capture the semantics of
084 individual movement. Others use raw GPS coordinates (e.g., UniTraj Zhu et al. (2024)), which are
085 too fragmented to represent daily routines, or rely on city-specific Zone IDs (e.g., TrajGPT Hsu et al.
086 (2024), UniMob Long et al. (2024), GenMove Long et al. (2025a)), which are not universal and
087 prevent the creation of large-scale, cross-city pre-training datasets. The second barrier is architectural.
088 Human mobility, much like language, is a mixture of distinct behaviors shaped by varied intents and
089 geographical contexts Han et al. (2025). Existing models, with their “one-fits-all” parameters, are
090 forced to learn an inefficient, averaged representation of these diverse patterns, failing to capture
091 the rich semantics of movement as data diversity grows. Recent LLM-based approaches (Wang
092 et al., 2023; Li et al., 2024a; Feng et al., 2025; Du et al., 2024; 2025) sidestep this by reasoning in a
language space, a process that divorces the model from the data’s intrinsic spatio-temporal structure.

093 In this work, we introduce MoveGPT, a scalable and unified architecture for pre-training large-scale
094 foundation models on massive human mobility datasets. To address the representation challenge,
095 MoveGPT introduces a unified location encoder that maps all locations into a universal semantic
096 feature space based on their geographic, functional, and social characteristics. This unlocks the ability
097 to pool large-scale datasets, enabling us to construct a pre-training corpus of unprecedented scale.
098 To tackle the architectural challenge, we design MoveGPT as a decoder-only Transformer with a
099 Spatially-Aware Mixture-of-Experts (SAMoE) architecture. This allows to develop specialized sub-
100 networks (“experts”) for distinct spatial contexts and behavioral patterns, efficiently learning a rich
101 understanding of movement as data scales. Operating in an auto-regressive manner, this framework is
102 inherently flexible, supporting various tasks and prediction horizons. Pre-trained on a massive dataset
103 of over 1.5 billion samples from more than 16 cities, MoveGPT establishes a new state-of-the-art on
104 a wide range of downstream tasks and demonstrates remarkable generalization ability to new cities.
105 Further analysis confirms the model’s ability to create a unified urban feature space while capturing
106 the hierarchical nature of human mobility. Our work provides empirical evidence of scaling ability
107 in human mobility, demonstrating predictable performance gains from data volume, model size,
and data diversity. This validates a clear and principled path toward building increasingly capable
foundation models for human mobility. Our key contributions are as follows:

- To our best knowledge, we are the first to scale mobility foundation models by tackling the dual barriers of location heterogeneity across geographies and pattern heterogeneity in behaviors.
- We introduce MoveGPT, a novel architecture featuring a unified location encoder for global-scale representation and spatially-aware mixture-of-experts Transformers to efficiently model diverse movement patterns.
- MoveGPT establishes a new state-of-the-art on a wide range of downstream tasks, with improvements of up to 30% in prediction and 80% in generation. We present empirical evidence of scaling ability in human mobility.

2 PRELIMINARY

Human mobility data. Human mobility datasets record the movement trajectories of individuals. Unlike raw GPS data which records continuous movement, our work focuses on trajectories composed of semantically meaningful stay points, which are significant locations where an individual spends time. An individual’s movement trajectory S_u is thus represented as a time-ordered sequence of these stay points:

$$S_u = \langle \tilde{t}_1, loc_1 \rangle, \langle \tilde{t}_2, loc_2 \rangle, \dots, \langle \tilde{t}_n, loc_n \rangle \quad (1)$$

where \tilde{t}_i denotes the timestamp and loc_i is the i-th stay point, forming an irregular time series. For computational representation, each unique location loc_i is mapped to a cell within a non-overlapping grid. Furthermore, we enrich each location with high-level features (e.g., functionality and geographical attributes) to achieve a more expressive representation.

General mobility modeling. To comprehensively evaluate our model’s capabilities, we address five fundamental tasks in human mobility modeling. These tasks provide complementary perspectives on understanding, simulating, and evaluating real-world movement behaviors: (1) **next-location prediction**: forecasting the next location based on a user’s historical trajectory; (2) **long-term prediction**: predicting a user’s trajectory over an extended future time horizon; (3) **unconditional generation**: generating realistic mobility trajectories that reflect typical movement patterns within a city; (4) **conditional generation**: generating trajectories that adhere to specific, given constraints or user attributes (e.g., a certain radius of gyration); (5) **anomaly detection**: identifying abnormal trajectories that deviate from established patterns, potentially due to issues like sensor malfunctions. Successfully addressing these diverse tasks is essential for advancing the development of truly general-purpose mobility foundation models.

3 METHODOLOGY

Figure 2 illustrates the overall architecture of our proposed MoveGPT. Panel (a) presents the autoregressive pretraining of mobility data, implemented with a decoder-only transformer enhanced by causal attention and a spatially-aware mixture-of-experts (SAMoE). Panel (b) shows the unified encoding of locations across different cities. Panel (c) depicts how feature embeddings of all city locations are processed through a Deep & Cross Net to generate candidate embeddings, which facilitates a scalable location selection.

3.1 UNIFIED LOCATION ENCODER

Existing approaches typically rely on discrete IDs to encode locations. However, such representations hinder cross-city transferability. To build a mobility foundation model, it is essential to develop a unified encoder that can generate consistent representations of locations across different cities. Existing research (Hu et al., 2020; Song et al., 2010c; Gonzalez et al., 2008; Lenormand et al., 2020) shows evidence that human mobility is influenced by individual intents, travelers tend to choose their next destination based on travel needs and spatial distance. To capture this behavior, we use the locations’ functional feature (POI distribution) and geographic feature (geographic coordinates) as core features for the encoder. In addition, mobility patterns are also influenced by broader social dynamics. To account for this, we incorporate the social popularity level of each location as another key feature. Formally, for all locations in a city, we construct three embeddings:

$$\mathbf{E}_{POI} = \text{MLP}(\mathcal{P}), \mathbf{E}_{Geo} = \text{MLP}(\mathcal{G}), \mathbf{E}_{pop} = \text{MLP}(\mathcal{R}) \quad (2)$$

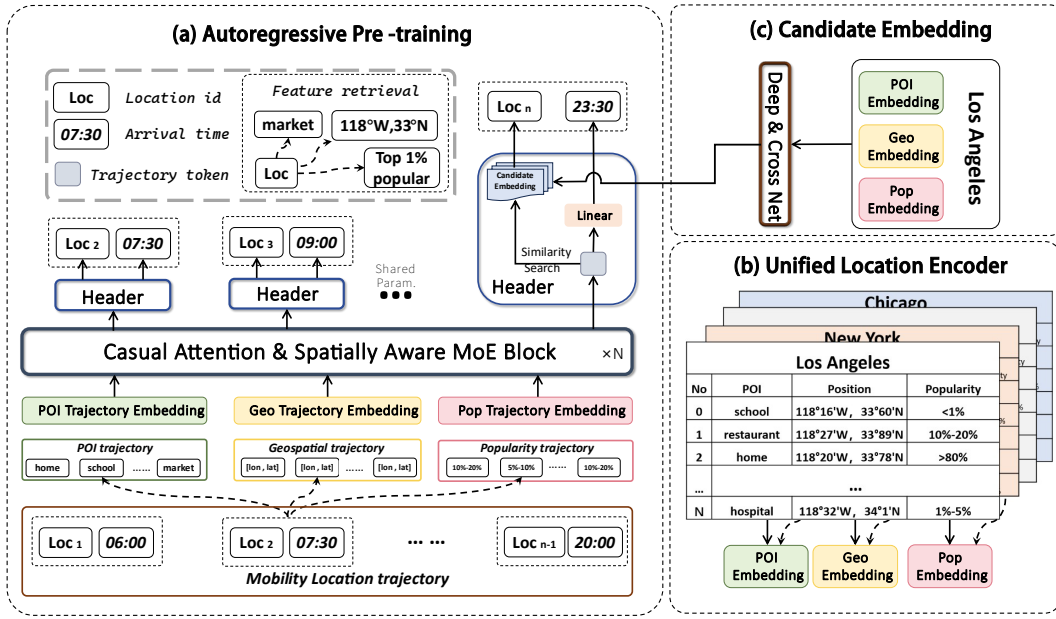


Figure 2: Illustration of the whole framework of MoveGPT, including three key components: (a) Autoregressive pretraining for mobility modeling; (b) Unified location encoder; (c) Candidate embedding for similarity search.

which \mathcal{P}, \mathcal{G} and \mathcal{R} represent POI distribution, geographic coordinates, and popularity level of the location. This encoding strategy not only preserves the uniqueness of each location but also projects spatial representations from different cities into a shared feature space, thereby enabling more effective and transferable modeling.

3.2 SPATIALLY-AWARE MIXTURE-OF-EXPERTS TRANSFORMER

To build mobility foundation models, another key challenge lies in the heterogeneity of individual mobility patterns. To address this, we design spatially-aware mixture-of-experts (SAMoE) Transformers, which leverage causal attention to capture the sequential patterns of mobility trajectories. The key departure from conventional MoE architectures is our spatially-aware routing mechanism, which intelligently assigns trajectory segments to specialized experts based on their spatial context and semantics.

Semantic-Aware Sequence Input. The mobility trajectory $S_u = \{loc_1, loc_2, \dots, loc_n\}$ is mapped into three new sequences through the location feature retrieval method illustrated in Figure 2:

$$S_f = \{x_1, x_2, \dots, x_n\}, \text{ where } x_i = (\text{POI}_i, \text{Geo}_i, \text{Pop}_i). \quad (3)$$

Each sequence is individually embedded to obtain E_{poi} , E_{geo} , and E_{pop} . The fused trajectory embedding is initialized as:

$$E_{\text{traj}} = E_{\text{poi}} + E_{\text{geo}} + E_{\text{pop}}. \quad (4)$$

Additionally, temporal information of the trajectory is embedded into E_{ts} , defined as:

$$E_{\text{ts}} = \text{EMB}(tod) + \text{EMB}(dow) + \text{EMB}(dur), \quad (5)$$

where $\text{Emb}(\cdot)$ denotes an embedding layer, tod is the time of day, dow is the day of week, and dur is the stay duration. E_{ts} replaces the traditional positional encoding in Transformer architectures. It is combined with trajectory embeddings (e.g., E_{traj}) and serves as input to the attention layers. As shown in Figure 3, fused trajectory embedding E_{traj} and three foundation sequence embedding ($E_{\text{poi}}, E_{\text{geo}}, E_{\text{pop}}$) are processed separately by causal attention layer and through residual connections and layer normalization, to obtain the token representations H of the four trajectories as input to the SAMoE block.

$$H_i = \text{CASUAL ATTENTION}(E_i), \text{ where } i \in (\text{traj}, \text{poi}, \text{geo}, \text{pop}). \quad (6)$$

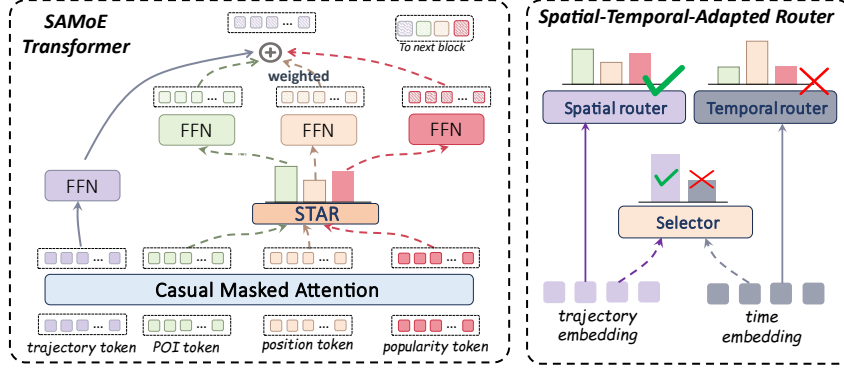


Figure 3: SAMoE Transformer block and SpatiaL-Temporal-Adapted Router(STAR).

Spatially-Aware Mixture-of-Experts. Human mobility is not driven by a single, monolithic principle. Instead, an individual’s movement results from a complex mixture of different intentions and constraints. For example, some movements are driven by personal preference and location function (e.g., choosing a specific restaurant, captured by POI features), while others are primarily sensitive to distance and travel cost (governed by geographic proximity). A third factor is social influence, where individuals are drawn to popular locations (reflected by popularity features). A single, monolithic model would be forced to learn an inefficient, averaged representation of these often-competing drivers. To address this, we design a Spatially-Aware Mixture-of-Experts framework. As illustrated in Figure 3, we instantiate separate experts to specialize in each of these core mobility drivers: a POI expert, a Geo expert, and a Pop expert. These experts operate in parallel, and their outputs are dynamically combined by a Spatial-Temporal-Adapted Router (STAR). STAR acts as a gating mechanism, analyzing the current trajectory context to adaptively weight the influence of each expert for the final prediction, thereby capturing the heterogeneous nature of real-world mobility decisions. STAR’s operation can be formally expressed as:

$$\begin{aligned} g_s^i &= \mathbf{W}_s^i(E_{\text{traj}}), \quad g_t^i = \mathbf{W}_t^i(E_{\text{ts}}) \\ [w_1, w_2] &= \text{MLP}(E_{\text{traj}} \| E_{\text{ts}}), \quad w = \begin{cases} 1, & \text{if } w_1 \geq w_2 \\ 0, & \text{otherwise} \end{cases} \\ g_i &= w \cdot g_s^i + (1 - w) \cdot g_t^i \end{aligned} \quad (7)$$

where \mathbf{W} is a learnable parameter matrix. g_s and g_t denote the feature importance scores provided by the spatial router and the temporal router, while w serves as an adaptive router selector. The overall formulation of SAMoE block can be expressed as:

$$\begin{aligned} \mathbf{g} &= \text{STAR}(\mathcal{H}_{\text{traj}}, E_{\text{ts}}), \\ H'_{\text{traj}} &= \text{FFN}_{\text{shared}}(H_{\text{traj}}) + \sum_i \mathbf{g}_i \text{FFN}_i(H_i). \quad \forall i \in \{\text{poi}, \text{geo}, \text{pop}\} \end{aligned} \quad (8)$$

3.3 NEXT-STEP OUTPUT

The final output layer is also a major bottleneck in scaling mobility models. Traditional approaches that use an MLP to produce a softmax distribution over all possible locations are inherently non-scalable, as the output dimension is fixed and cannot adapt to new or changing locations. To overcome this, we design a flexible and scalable pre-training task based on a retrieval framework.

Instead of direct classification, we model next-step prediction as a similarity search problem. Specifically, a mobility trajectory S is encoded by the SAMoE Transformer to produce a trajectory representation $H_{\text{traj}}^l \in \mathbb{R}^d$ for a given length l , which acts as a query. Concurrently, we create a candidate database $\mathcal{D} \in \mathbb{R}^{N \times d}$ containing embeddings for all N locations in the city, generated by a Deep & Cross Network (DCN) Wang et al. (2017) from their features (E_{poi} , E_{geo} , E_{pop}) as follows:

270
271
272

$$\mathcal{D} = \text{DCN}(E_{poi} + E_{geo} + E_{pop}) \quad (9)$$

273 loc^n is then determined by the dot-product similarity between the trajectory query and the candidate
274 embedding:
275

$$\hat{loc}^n = H_{\text{traj}}^l \cdot d^n, \quad d \in \mathcal{D} \quad (10)$$

276 This retrieval-based method is highly scalable, as the set of candidate locations \mathcal{D} can be updated
277 (e.g., adding new points of interest) without any changes to the core MoveGPT architecture. The
278 probability distribution for the next timestamp is generated by a linear layer.
281282 3.4 MODEL TRAINING
283284 We pretrain MoveGPT in an autoregressive manner on large-scale, multi-city mobility trajectories.
285 The fundamental task is next-step prediction: for any given trajectory, the model learns to predict
286 the next location and its corresponding timestamp. This joint objective enables the model to simul-
287 taneously capture the complex spatial patterns and temporal dynamics inherent in human mobility.
288 The overall training objective is therefore defined as the sum of the cross-entropy losses for both the
289 location and timestamp predictions:
290

$$\mathcal{L}_{\text{Loss}} = - \sum_{l=1}^T \sum_{n=1}^N loc_{l+1}^n \log \hat{loc}_{l+1}^n - \sum_{l=1}^T \sum_{m=1}^M t_{l+1}^m \log \hat{t}_{l+1}^m. \quad (11)$$

295 4 EXPERIMENTS
296297 We conduct extensive experiments to comprehensively evaluate MoveGPT. We pre-train two versions
298 of our model: MoveGPT_{base}, trained on one billion samples from six U.S. cities with a 4-layer
299 SAMoE Transformer, and MoveGPT_{ultra}, a larger model trained on 1.5 billion from 16 U.S. cities
300 with a 12-layer architecture. Further details on training and model configurations are available in
301 Appendix D.2.302 Our evaluation is comprehensive, addressing the model’s capabilities from multiple angles. We first
303 assess its cross-task generalization on a diverse range of downstream tasks, including next-location
304 prediction, long-term prediction, conditional/unconditional generation, and anomaly detection. We
305 then investigate the model’s scalability, analyzing its performance as we increase data volume,
306 model size, and the number of cities to test for scaling laws. Furthermore, we examine its transfer
307 learning capabilities to see how effectively it transfers learned knowledge to new cities with minimal
308 fine-tuning data. Finally, we conduct an in-depth analysis of the model’s internal mechanisms to
309 understand what the model has learned, and how it achieves a unified modeling.310 Detailed information on the used dataset, baselines, and model setup is provided in the Appendix C
311 and Appendix D. Further analyses, including ablation studies and additional results, can be found in
312 Appendix E.
313314 4.1 BASE TASK: NEXT LOCATION PREDICTION
315316 **Setups.** We compare our multi-city pre-trained models (MoveGPT_{base} and MoveGPT_{ultra}) against
317 state-of-the-art (SOTA) baselines across six major cities. To isolate the benefits of multi-city training
318 versus architectural superiority, we also train a single-city version, **MoveGPT (separate)**, for each
319 city. Performance is measured using Accuracy@k ($Acc@k$).320 **Results.** As shown in Table 2, MoveGPT decisively sets a new state-of-the-art. Notably, joint
321 training on multi-city data provides a significant performance boost of nearly 10% over the single-city
322 versions. This confirms that MoveGPT effectively learns transferable, universal mobility patterns
323 while still capturing city-specific heterogeneity. Moreover, even the single-city MoveGPT achieves
SOTA or near-SOTA results, demonstrating the inherent power of the SAMoE architecture itself.

Table 2: Comparison of MoveGPT against state-of-the-art baselines on Acc@1 and Acc@3. The **best** and **second-best** results in each column are highlighted.

City	Atlanta		Chicago		Seattle		Washington		New York		Los Angeles		Average	
Metric	Acc@1	Acc@3												
Markov	0.133	0.300	0.123	0.264	0.125	0.249	0.123	0.326	0.109	0.296	0.102	0.235	0.119	0.278
LSTM	0.181	0.356	0.178	0.353	0.174	0.343	0.185	0.371	0.176	0.348	0.143	0.336	0.172	0.351
Transformer	0.164	0.337	0.160	0.317	0.158	0.324	0.159	0.345	0.163	0.355	0.135	0.327	0.156	0.334
DeepMove	0.184	0.384	0.168	0.343	0.171	0.346	0.186	0.375	0.165	0.345	0.151	0.338	0.171	0.355
GetNext	0.190	0.375	0.186	0.364	0.186	0.363	0.203	0.394	0.183	0.366	0.159	0.334	0.184	0.366
CTLE	0.206	0.403	0.183	0.361	0.194	0.371	0.192	0.378	0.163	0.349	0.150	0.336	0.181	0.366
TrajFM	0.208	0.402	0.191	0.361	0.209	0.381	0.201	0.407	0.186	0.372	0.155	0.337	0.192	0.377
UniMove	0.217	0.361	0.209	0.360	0.235	0.393	0.232	0.378	0.214	0.338	0.171	0.259	0.213	0.348
TrajGPT	0.214	0.400	0.203	0.361	0.226	0.390	0.225	0.386	0.192	0.366	0.179	0.320	0.206	0.370
Unitraj	0.222	0.402	0.197	0.362	0.223	0.391	0.214	0.410	0.196	0.374	0.181	0.339	0.205	0.380
MoveGPT(ours)														
<i>separate</i>	0.249	0.400	0.236	0.363	0.265	0.425	0.254	0.403	0.235	0.374	0.221	0.336	0.243	0.383
<i>base</i>	0.272	0.428	0.258	0.392	0.283	0.447	0.277	0.432	0.261	0.407	0.241	0.363	0.265	0.411
<i>ultra</i>	0.293	0.430	0.272	0.407	0.295	0.451	0.297	0.430	0.274	0.428	0.237	0.368	0.278	0.419

4.2 GENERALIZATION TO DOWNSTREAM MOBILITY TASKS

To demonstrate its generalization as a foundation model, we evaluate MoveGPT on a diverse set of downstream tasks: long-term prediction, mobility generation, and anomaly detection.

Long Term Prediction. This task tests the model’s ability to capture long-range dependencies by predicting an entire day’s trajectory based on the previous day. While baseline models suffer from rapidly accumulating errors over longer prediction horizons, MoveGPT’s performance remains robust. It outperforms all baselines, achieving average gains of 45% on Acc@1 and 18% on Acc@3. This showcases its superior ability to model long-range spatiotemporal patterns, a critical requirement for multi-step forecasting.

Unconditional Generation. Here, the goal is to generate realistic, unprompted daily trajectories that capture the natural patterns of a city. We prompted MoveGPT with random starting points and times to autoregressively generate one-day mobility sequences. To measure realism, we assessed the similarity between generated and real trajectories using Jensen-Shannon Divergence (JSD) across three key attribute distributions: single-trip distance, dwell time, and radius of gyration. As shown in Table 3, MoveGPT’s generated trajectories are significantly more realistic than those from baselines, yielding an average **65% improvement** in JSD in cities like Atlanta, Chicago, and Seattle. This result demonstrates that MoveGPT has learned a deep and accurate understanding of the underlying mobility data distribution.

Conditional Generation. This more challenging task tests the model’s ability to generate trajectories that adhere to a specific, user-defined constraint—in this case, a given radius of gyration. The model must reconcile this explicit constraint with realistic mobility patterns. We evaluate performance on two criteria: realism (JSD of the resulting distribution) and adherence (Mean Absolute Error in km between the target and realized radius of gyration). As detailed in Table 8 of Appendix E.3, MoveGPT demonstrates remarkable control. On average, it reduces the JSD by **40%** and the MAE by **27%** compared to baselines. This confirms MoveGPT’s advanced capability to generate not just realistic but also steerable and controllable mobility patterns.

Anomalous Detection. Finally, we test if MoveGPT’s understanding of normal patterns can be leveraged for anomaly detection. By using its learned representations to identify trajectories that deviate from the norm, MoveGPT achieves significant performance improvements over baselines (Appendix

378
 379 Table 3: Performance of unconditional mobility generation, measured by JSD for trip **Distance**, stay
 380 **Duration**, and **Radius** of gyration (**lower is better**). The **best** and **second-best** results are highlighted.

381 City	Atlanta			Chicago			Seattle			Washington			New York			Average		
	382 Models	Dis.	Dur.	Rad.	383 Dis.	Dur.	Rad.	384 Dis.	Dur.	Rad.	385 Dis.	Dur.	Rad.	386 Dis.	Dur.	Rad.	387 Dis.	Dur.
TrajGAN	0.353	0.214	0.079	0.302	0.360	0.807	0.406	0.169	0.354	0.209	0.151	0.127	0.184	0.187	0.207	0.291	0.216	0.315
DiffLSTM	0.203	0.100	0.045	0.150	0.200	0.304	0.182	0.089	0.180	0.093	0.078	0.079	0.088	0.096	0.119	0.143	0.112	0.145
Movesim	0.221	0.119	0.054	0.163	0.225	0.320	0.201	0.092	0.202	0.101	0.080	0.083	0.096	0.097	0.115	0.156	0.122	0.155
Difftraj	0.121	0.057	0.017	0.097	0.121	0.221	0.126	0.040	0.089	0.058	0.036	0.042	0.045	0.044	0.054	0.089	0.060	0.084
Unitraj	0.112	0.226	0.153	0.068	0.259	0.203	0.162	0.205	0.172	0.066	0.214	0.205	0.071	0.268	0.219	0.095	0.234	0.190
MoveGPT _{base}	0.025	0.042	0.017	0.037	0.043	0.051	0.052	0.033	0.026	0.051	0.048	0.031	0.044	0.035	0.059	0.041	0.040	0.037
MoveGPT _{ultra}	0.021	0.034	0.016	0.029	0.037	0.031	0.045	0.021	0.026	0.044	0.039	0.028	0.037	0.022	0.056	0.029	0.025	0.026

393 Table 9), with gains of approximately **17% in precision and 8% in recall**. This demonstrates that
 394 the pre-trained model has implicitly learned a powerful and robust representation of normal human
 395 mobility. The fine-tuning settings are shown in Appendix D.3.

397 4.3 SCALABILITY ANALYSIS

399 We conduct a comprehensive analysis of the scalability of our model from three perspectives: (1)
 400 **Data Volume**: increasing the amount of training data while keeping the number of training cities
 401 fixed; (2) **Model Parameter**: varying the model parameters under the same training data; (3) **Data**
 402 **Diversity**: starting from a single-city dataset and progressively incorporating additional cities to
 403 enrich the diversity of individual mobility patterns. As illustrated in Appendix Figure 9, larger model
 404 capacity and a larger amount of training data consistently lead to improved performance, which is
 405 consistent with the general understanding of foundation models. Moreover, MoveGPT effectively
 406 handles the heterogeneity of mobility data across cities, and incorporating more diverse mobility
 407 trajectories during training yields substantial performance gains.

408 4.4 TRANSFER LEARNING

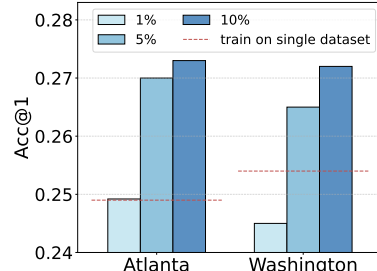
410 One significant advantage of employing large-scale data for
 411 model pretraining lies in the effective transfer of knowledge
 412 acquired from pretraining datasets to target cities. This enables
 413 the model to achieve superior prediction performance through
 414 minimal data fine-tuning in target domains. To systematically
 415 validate the model’s generalization capability, we conducted
 416 experiments with 1%, 5%, and 10% of target city data for
 417 single-epoch fine-tuning on the pretrained model. As illus-
 418 trated in Figure 4, the results demonstrate that merely 5% of
 419 data for fine-tuning can **outperform** the performance achieved
 420 by training non-pretrained models with **full** datasets. This com-
 421 pelling evidence substantiates the exceptional generalization capacity of our pretraining methodology,
 422 highlighting its effectiveness in cross-city knowledge transfer with limited target data requirements.

423 4.5 IN-DEPTH MODEL ANALYSIS

425 To understand the sources of MoveGPT’s strong performance, we conduct an in-depth analysis of its
 426 key components. We aim to “open the black box” to interpret what the model has learned and how it
 427 handles the complexities of multi-city mobility data.

429 4.5.1 INTERPRETING THE SPATIOTEMPORAL ROUTING MECHANISM

431 We first analyze the behavior of the Spatial-Temporal-Adapted Router (STAR) to understand how it
 432 processes mobility patterns.



433 Figure 4: Transfer performance on
 434 new cities.

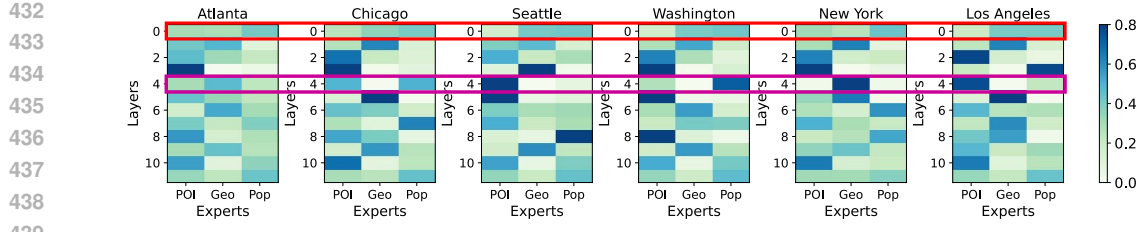


Figure 5: The distribution of the spatial router’s weights across different layers in MoveGPT shows both cross-city similarities (e.g., the first layer highlighted in red) and city-specific characteristics (e.g., the fourth layer highlighted in purple).

Spatial Router Analysis. As shown in Figure 5, the spatial router’s weights reveal a distinct hierarchical learning pattern across its layers. We observe that the initial and final layers focus on capturing a mixture of fundamental features (geography, POI, popularity). In contrast, the intermediate layers specialize in more abstract semantic patterns, such as complex sequential dependencies and contextual transitions. This layered specialization indicates that MoveGPT effectively integrates low-level spatial data with high-level semantic information to build robust mobility representations.

Temporal Router Analysis. The temporal router, analyzed in Appendix Figure 8, shows a predominant and consistent focus on POI semantics across most times of the day and in different cities. This suggests that the model learns that the functional purpose of a location (e.g., dining, working), represented by POIs, is a more stable and powerful indicator of human temporal patterns than mere geographic coordinates.

4.5.2 ALIGNMENT OF LOCATION REPRESENTATIONS

A key hypothesis of our work is that a unified location encoder can learn shared spatial semantics across cities. To validate this, we analyze the location embedding layer before and after pre-training. As visualized in Figure 6, the pre-training process transforms the initially scattered, city-specific embeddings into a much more aligned and unified feature space where locations with similar characteristics from different cities cluster together. This provides direct evidence that our encoder successfully bridges the gap between heterogeneous urban environments, which is critical for the model’s strong cross-city generalization capabilities.

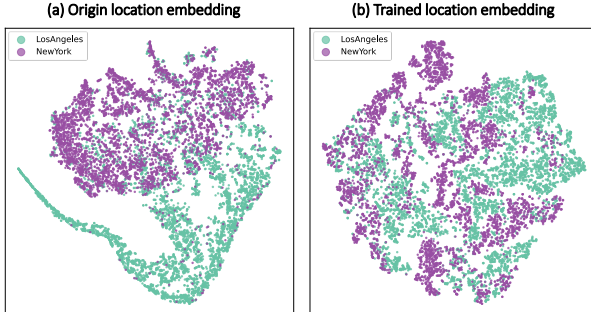


Figure 6: t-SNE visualization of location embeddings for Los Angeles and Chicago: (a) original embeddings before training, and (b) final embeddings after training.

5 CONCLUSION

In this paper, we introduce MoveGPT, a large-scale foundation model that represents a paradigm shift in human mobility research, moving the field beyond the era of fragmented, task-specific models and ushering in a new age of general-purpose, foundational systems. Crucially, our work provides the first empirical evidence of scaling laws in human mobility. We demonstrate that, analogous to the domain of natural language, performance predictably improves with increases in data volume, model size, and data diversity. The implications of MoveGPT extend far beyond academic benchmarks. By laying a robust and scalable foundation, it paves the way for transformative applications in intelligent urban planning, dynamic traffic management, and proactive public health responses. MoveGPT not only advances the state-of-the-art but also charts a clear course for the future of mobility intelligence, promising a deeper, more actionable understanding of the complex dynamics that shape our world.

486 **ETHICS STATEMENT**

487

488 The authors have adhered to the ICLR Code of Ethics in the conduct of this research. Our primary
 489 ethical considerations were data privacy and the prevention of bias. To protect the privacy of data
 490 subjects, we have implemented several robust measures. The dataset used in this study is fully
 491 anonymized and contains no personally identifiable information (PII). To further enhance privacy,
 492 random noise is added to all location data points (a technique known as location perturbation), making
 493 the re-identification of individuals infeasible. Furthermore, the dataset is stored on a secure, encrypted
 494 server with access strictly limited to authorized research personnel. Our dataset does not contain any
 495 demographic or user-specific attributes, such as gender, race, or age. It inherently mitigates the risk
 496 of our model learning and perpetuating societal biases related to these protected characteristics.

497 Beyond mitigating potential risks, we believe this research has significant positive societal implications.
 498 As a foundational tool, MoveGPT is poised to help address major challenges in intelligent
 499 urban planning, transportation systems, and public health. We are committed to fostering our research
 500 to ensure it contributes constructively to these vital domains.

501

502 **REPRODUCIBILITY STATEMENT**

503

504 In line with our commitment to open and reproducible science, all artifacts required to validate our
 505 findings are provided. This includes the complete source code for model training and evaluation,
 506 pre-trained model weights, and all configuration files. These materials are available in an anonymized
 507 public repository <https://anonymous.4open.science/r/MoveGPT-FC72/> to allow for
 508 the verification and extension of our work by the community.

509

510 **REFERENCES**

511

- 512 Jianwei Chen, Jianbo Li, and Ying Li. Predicting human mobility via long short-term patterns.
Computer Modeling in Engineering & Sciences, 124(3):847–864, 2020.
- 514 Chen Chu, Hengcai Zhang, and Feng Lu. Trajgdm: A new trajectory foundation model for simulating
 515 human mobility. In *Proceedings of the 31st ACM International Conference on Advances in
 516 Geographic Information Systems*, pp. 1–2, 2023.
- 517 Riccardo Corrias, Martin Gjoreski, and Marc Langheinrich. Exploring transformer and graph
 518 convolutional networks for human mobility modeling. *Sensors*, 23(10):4803, 2023.
- 520 Nan Du, Yanping Huang, Andrew M Dai, Simon Tong, Dmitry Lepikhin, Yuanzhong Xu, Maxim
 521 Krikun, Yanqi Zhou, Adams Wei Yu, Orhan Firat, et al. Glam: Efficient scaling of language models
 522 with mixture-of-experts. In *International conference on machine learning*, pp. 5547–5569. PMLR,
 523 2022.
- 524 Yuwei Du, Jie Feng, Jie Zhao, and Yong Li. Trajagent: An agent framework for unified trajectory
 525 modelling. *arXiv e-prints*, pp. arXiv–2410, 2024.
- 527 Yuwei Du, Jie Feng, Jian Yuan, and Yong Li. Cams: A citygpt-powered agentic framework for urban
 528 human mobility simulation. *arXiv preprint arXiv:2506.13599*, 2025.
- 529 William Fedus, Barret Zoph, and Noam Shazeer. Switch transformers: Scaling to trillion parameter
 530 models with simple and efficient sparsity. *Journal of Machine Learning Research*, 23(120):1–39,
 531 2022.
- 533 Jie Feng, Yong Li, Chao Zhang, Funing Sun, Fanchao Meng, Ang Guo, and Depeng Jin. Deepmove:
 534 Predicting human mobility with attentional recurrent networks. In *WWW*, pp. 1459–1468, 2018.
- 535 Jie Feng, Zeyu Yang, Fengli Xu, Haisu Yu, Mudan Wang, and Yong Li. Learning to simulate
 536 human mobility. In *Proceedings of the 26th ACM SIGKDD international conference on knowledge
 537 discovery & data mining*, pp. 3426–3433, 2020.
- 539 Jie Feng, Yuwei Du, Jie Zhao, and Yong Li. Agentmove: Predicting human mobility anywhere using
 540 large language model based agentic framework. *NAACL*, 2025.

- 540 Sébastien Gambs, Marc-Olivier Killijian, and Miguel Núñez del Prado Cortez. Next place prediction
 541 using mobility markov chains. In *Proceedings of the first workshop on measurement, privacy, and*
 542 *mobility*, pp. 1–6, 2012.
- 543
- 544 Marta C Gonzalez, Cesar A Hidalgo, and Albert-Laszlo Barabasi. Understanding individual human
 545 mobility patterns. *nature*, 453(7196):779–782, 2008.
- 546 Ian J Goodfellow, Jean Pouget-Abadie, Mehdi Mirza, Bing Xu, David Warde-Farley, Sherjil Ozair,
 547 Aaron Courville, and Yoshua Bengio. Generative adversarial nets. *Advances in neural information*
 548 *processing systems*, 27, 2014.
- 549 Alex Graves. Long short-term memory. *Supervised sequence labelling with recurrent neural networks*,
 550 pp. 37–45, 2012.
- 552 Chonghua Han, Yuan Yuan, Yukun Liu, Jingtao Ding, Jie Feng, and Yong Li. Unimove: A unified
 553 model for multi-city human mobility prediction. *arXiv preprint arXiv:2508.06986*, 2025.
- 554 Shang-Ling Hsu, Emmanuel Tung, John Krumm, Cyrus Shahabi, and Khurram Shafique. Trajgpt:
 555 Controlled synthetic trajectory generation using a multitask transformer-based spatiotemporal
 556 model. In *Proceedings of the 32nd ACM International Conference on Advances in Geographic*
 557 *Information Systems*, pp. 362–371, 2024.
- 559 Yanan Hu, Wen-Xu Wang, Yong-Sheng Li, Ming-Sheng Chen, and Jing Lu. A universal op-
 560 portunity model for human mobility. *Scientific Reports*, 10(1):4820, 2020. doi: 10.1038/
 561 s41598-020-61845-x.
- 562 Robert A Jacobs, Michael I Jordan, Steven J Nowlan, and Geoffrey E Hinton. Adaptive mixtures of
 563 local experts. *Neural computation*, 3(1):79–87, 1991.
- 565 Shan Jiang, Yingxiang Yang, Siddharth Gupta, Daniele Veneziano, Shounak Athavale, and Marta C
 566 González. The timegeo modeling framework for urban mobility without travel surveys. *Proceedings*
 567 *of the National Academy of Sciences*, 113(37):E5370–E5378, 2016.
- 568 Michael I Jordan and Robert A Jacobs. Hierarchical mixtures of experts and the em algorithm. *Neural*
 569 *computation*, 6(2):181–214, 1994.
- 571 Maxime Lenormand, Mario Roy, Lajos Z Gergely, Marie-Louise Roy, Stefano D’Aronco, Nico-
 572 las Perret, David Alet, and José J Ramasco. On the importance of trip destination for
 573 modelling individual human mobility patterns. *Scientific Reports*, 10(1):17822, 2020. doi:
 574 10.1038/s41598-020-74528-7.
- 575 Dmitry Lepikhin, HyoukJoong Lee, Yuanzhong Xu, Dehao Chen, Orhan Firat, Yanping Huang,
 576 Maxim Krikun, Noam Shazeer, and Zhifeng Chen. Gshard: Scaling giant models with conditional
 577 computation and automatic sharding. In *International Conference on Learning Representations*.
- 578 Xuchuan Li, Fei Huang, Jianrong Lv, Zhixiong Xiao, Guolong Li, and Yang Yue. Be more real:
 579 Travel diary generation using llm agents and individual profiles. *arXiv preprint arXiv:2407.18932*,
 580 2024a.
- 582 Zhonghang Li, Lianghao Xia, Jiabin Tang, Yong Xu, Lei Shi, Long Xia, Dawei Yin, and Chao Huang.
 583 Urbangpt: Spatio-temporal large language models. In *Proceedings of the 30th ACM SIGKDD*
 584 *Conference on Knowledge Discovery and Data Mining*, pp. 5351–5362, 2024b.
- 585 Yan Lin, Huaiyu Wan, Shengnan Guo, and Youfang Lin. Pre-training context and time aware location
 586 embeddings from spatial-temporal trajectories for user next location prediction. In *Proceedings of*
 587 *the AAAI conference on artificial intelligence*, volume 35, pp. 4241–4248, 2021.
- 588 Yan Lin, Tonglong Wei, Zeyu Zhou, Haomin Wen, Jilin Hu, Shengnan Guo, Youfang Lin, and Huaiyu
 589 Wan. Trajfm: A vehicle trajectory foundation model for region and task transferability. *arXiv*
 590 *preprint arXiv:2408.15251*, 2024.
- 592 Aixin Liu, Bei Feng, Bin Wang, Bingxuan Wang, Bo Liu, Chenggang Zhao, Chengqi Dengr, Chong
 593 Ruan, Damai Dai, Daya Guo, et al. Deepseek-v2: A strong, economical, and efficient mixture-of-
 experts language model. *arXiv preprint arXiv:2405.04434*, 2024.

- 594 Yiding Liu, Kaiqi Zhao, Gao Cong, and Zhifeng Bao. Online anomalous trajectory detection
 595 with deep generative sequence modeling. In *2020 IEEE 36th International Conference on Data*
 596 *Engineering (ICDE)*, pp. 949–960. IEEE, 2020.
- 597 Qingyue Long, Yuan Yuan, and Yong Li. A universal model for human mobility prediction. *arXiv*
 598 *preprint arXiv:2412.15294*, 2024.
- 600 Qingyue Long, Can Rong, Huandong Wang, and Yong Li. One fits all: General mobility trajectory
 601 modeling via masked conditional diffusion. *arXiv preprint arXiv:2501.13347*, 2025a.
- 602 Qingyue Long, Yuan Yuan, and Yong Li. A universal model for human mobility prediction. In
 603 *Proceedings of the 31st ACM SIGKDD Conference on Knowledge Discovery and Data Mining V*.
 604 *1*, pp. 894–905, 2025b.
- 605 Pankaj Malhotra, Anusha Ramakrishnan, Gaurangi Anand, Lovekesh Vig, Puneet Agarwal, and
 606 Gautam Shroff. Lstm-based encoder-decoder for multi-sensor anomaly detection. *arXiv preprint*
 607 *arXiv:1607.00148*, 2016.
- 609 Christian M Schneider, Vitaly Belik, Thomas Couronné, Zbigniew Smoreda, and Marta C González.
 610 Unravelling daily human mobility motifs. *Journal of The Royal Society Interface*, 10(84):20130246,
 611 2013.
- 612 Noam Shazeer, Azalia Mirhoseini, Krzysztof Maziarz, Andy Davis, Quoc Le, Geoffrey Hinton, and
 613 Jeff Dean. Outrageously large neural networks: The sparsely-gated mixture-of-experts layer. *arXiv*
 614 *preprint arXiv:1701.06538*, 2017.
- 616 Junjun Si, Jin Yang, Yang Xiang, Hanqiu Wang, Li Li, Rongqing Zhang, Bo Tu, and Xiangqun
 617 Chen. Trajbert: Bert-based trajectory recovery with spatial-temporal refinement for implicit sparse
 618 trajectories. *IEEE Transactions on Mobile Computing*, 2023.
- 619 Chaoming Song, Tal Koren, Pu Wang, and Albert-László Barabási. Modelling the scaling properties
 620 of human mobility. *Nature physics*, 6(10):818–823, 2010a.
- 622 Chaoming Song, Zehui Qu, Nicholas Blumm, and Albert-László Barabási. Limits of predictability in
 623 human mobility. *Science*, 327(5968):1018–1021, 2010b.
- 624 Chaoming Song, Zehui Qu, Nicholas Blumm, and Albert-László Barabási. Universal scaling laws in
 625 human mobility. *Science*, 327(5967):1018–1021, 2010c. doi: 10.1126/science.1177170.
- 627 Hao Sun, Changjie Yang, Liwei Deng, Fan Zhou, Feiteng Huang, and Kai Zheng. Periodicmove:
 628 Shift-aware human mobility recovery with graph neural network. In *Proceedings of the 30th ACM*
 629 *International Conference on Information & Knowledge Management*, pp. 1734–1743, 2021.
- 630 Fernando Terroso-Sáenz and Andrés Muñoz. Nation-wide human mobility prediction based on graph
 631 neural networks. *Applied Intelligence*, pp. 1–17, 2022.
- 633 A Vaswani. Attention is all you need. *Advances in Neural Information Processing Systems*, 2017.
- 634 Ruoxi Wang, Bin Fu, Gang Fu, and Mingliang Wang. Deep & cross network for ad click predictions.
 635 In *Proceedings of the ADKDD’17*, pp. 1–7, 2017.
- 637 Xinglei Wang, Meng Fang, Zichao Zeng, and Tao Cheng. Where would i go next? large language
 638 models as human mobility predictors. *arXiv preprint arXiv:2308.15197*, 2023.
- 639 Hao Xue, Flora Salim, Yongli Ren, and Nuria Oliver. Mobtcast: Leveraging auxiliary trajectory
 640 forecasting for human mobility prediction. *Advances in Neural Information Processing Systems*,
 641 34:30380–30391, 2021.
- 642 Song Yang, Jiamou Liu, and Kaiqi Zhao. Getnext: trajectory flow map enhanced transformer for
 643 next poi recommendation. In *Proceedings of the 45th International ACM SIGIR Conference on*
 644 *research and development in information retrieval*, pp. 1144–1153, 2022.
- 646 Yuan Yuan, Jingtao Ding, Huandong Wang, Depeng Jin, and Yong Li. Activity trajectory generation
 647 via modeling spatiotemporal dynamics. In *Proceedings of the 28th ACM SIGKDD Conference on*
Knowledge Discovery and Data Mining, pp. 4752–4762, 2022.

- 648 Yuan Yuan, Jingtao Ding, Chenyang Shao, Depeng Jin, and Yong Li. Spatio-temporal diffusion point
649 processes. In *Proceedings of the 29th ACM SIGKDD Conference on Knowledge Discovery and*
650 *Data Mining*, pp. 3173–3184, 2023.
- 651
- 652 Yuan Yuan, Jingtao Ding, Jie Feng, Depeng Jin, and Yong Li. Unist: A prompt-empowered universal
653 model for urban spatio-temporal prediction. In *Proceedings of the 30th ACM SIGKDD Conference*
654 *on Knowledge Discovery and Data Mining*, pp. 4095–4106, 2024a.
- 655 Yuan Yuan, Chonghua Han, Jingtao Ding, Depeng Jin, and Yong Li. Urbandit: A foundation model
656 for open-world urban spatio-temporal learning. *arXiv preprint arXiv:2411.12164*, 2024b.
- 657
- 658 Yanqi Zhou, Tao Lei, Hanxiao Liu, Nan Du, Yanping Huang, Vincent Zhao, Andrew M Dai, Quoc V
659 Le, James Laudon, et al. Mixture-of-experts with expert choice routing. *Advances in Neural*
660 *Information Processing Systems*, 35:7103–7114, 2022.
- 661 Zhen Zhou, Ziyuan Gu, Xiaobo Qu, Pan Liu, Zhiyuan Liu, and Wenwu Yu. Urban mobility foundation
662 model: A literature review and hierarchical perspective. *Transportation Research Part E: Logistics*
663 *and Transportation Review*, 192:103795, 2024.
- 664
- 665 Yuanshao Zhu, Yongchao Ye, Shiyao Zhang, Xiangyu Zhao, and James Yu. Difftraj: Generating gps
666 trajectory with diffusion probabilistic model. *Advances in Neural Information Processing Systems*,
667 36:65168–65188, 2023.
- 668 Yuanshao Zhu, James Jianqiao Yu, Xiangyu Zhao, Xuetao Wei, and Yuxuan Liang. Unitraj: Universal
669 human trajectory modeling from billion-scale worldwide traces. *arXiv preprint arXiv:2411.03859*,
670 2024.
- 671
- 672
- 673
- 674
- 675
- 676
- 677
- 678
- 679
- 680
- 681
- 682
- 683
- 684
- 685
- 686
- 687
- 688
- 689
- 690
- 691
- 692
- 693
- 694
- 695
- 696
- 697
- 698
- 699
- 700
- 701

702 A USAGE OF LARGE LANGUAGE MODEL 703

704 We employed the Google Gemini large language model as an auxiliary writing tool for minor linguistic
705 refinements. Its use was strictly limited to proofreading and improving the grammatical clarity of the
706 text. The substantive content, including all ideas, methods, analyses, and conclusions, is entirely the
707 original work of the authors.

709 B RELATED WORK 710

711 B.1 HUMAN MOBILITY MODELING 712

713 Human mobility modeling encompasses a broad spectrum of tasks, including mobility prediction,
714 generation, and anomaly detection. These tasks jointly provide complementary perspectives for
715 understanding, simulating, and evaluating human movement behaviors (Song et al., 2010b; Schneider
716 et al., 2013). Early approaches were dominated by probabilistic models such as Markov chains
717 and exploration-preferential return (EPR) models (Gambs et al., 2012; Jiang et al., 2016), which
718 captured mobility patterns from transition probabilities but struggled with the irregular and dynamic
719 nature of human behavior. Recent advances in deep learning have significantly boosted the field, with
720 recurrent neural networks (RNNs) (Chen et al., 2020; Yuan et al., 2022), attention-based architectures
721 (Feng et al., 2018; Yuan et al., 2023), Transformers (Corrias et al., 2023; Si et al., 2023), graph
722 neural networks (GNNs) (Sun et al., 2021; Terroso-Sáenz & Muñoz, 2022), and diffusion models
723 (Zhu et al., 2023; Long et al., 2025a) being widely applied across different tasks. However, most of
724 these models remain city-specific, requiring separate training for each dataset and thus limiting their
725 generalizability. Inspired by the paradigm shift in natural language processing, a series of mobility
726 foundation models have recently been proposed, including UniST (Yuan et al., 2024a), UrbanDiT
727 (Yuan et al., 2024b), TrajFM (Lin et al., 2024), TrajGPT (Hsu et al., 2024), UniMob (Long et al.,
728 2025b), GenMove (Long et al., 2025a), and UniTraj (Zhu et al., 2024). These approaches attempt to
729 leverage large-scale pre-training to improve few-shot and zero-shot performance, yet most still can
730 not capture the universality and diversity of human mobility patterns across urban environments.

731 B.2 MIXTURE OF EXPERTS 732

733 Mixture of Experts (MoE) Shazeer et al. (2017); Jordan & Jacobs (1994); Jacobs et al. (1991) is a
734 deep learning architecture that enhances model performance through a divide-and-conquer strategy.
735 Its core idea lies in decomposing complex tasks and enabling collaborative processing by multiple
736 specialized sub-models (experts), guided by a learnable gating network that dynamically allocates
737 input data to the most relevant experts Zhou et al. (2022). Each expert processes only a subset of
738 inputs, significantly reducing computational costs, while the gating mechanism synthesizes final
739 results through weighted aggregation of expert outputs Fedus et al. (2022); Lepikhin et al.. By
740 maintaining the model’s parameter scale while improving inference efficiency, MoE has been widely
741 adopted in large-scale language models Liu et al. (2024); Du et al. (2022); Lepikhin et al., enabling
742 trillion-parameter model deployment via sparse activation. However, challenges such as expert load
743 balancing and training stability persist in its implementation.

744 C DATASET DETAILS 745

746 We provide detailed information about the dataset used in this study, as shown in the Table 4. The
747 dataset consists of approximately 1.5 billion trajectory points from 16 U.S. cities, each with different
748 population distributions, economic conditions, and urban structures. For pre-processing the trajectory
749 data in these datasets, the trajectory locations of each user are mapped to $500m \times 500m$ grid cells.
750 We applied a sliding window of three days to each user’s trajectory and filtered out trajectories with
751 fewer than five trajectory points. For every location, POI data is sourced from Open Street Map and
752 consists of 34 major categories ,and the details are shown in Table 5. The longitude and latitude
753 of all locations in the same city are normalized to have a mean of 0 and a standard deviation of 1.
754 We discrete the popularity rank based on quintiles, and details are shown in Tables 6. For temporal
755 pre-processing, we divide a day into 48 time slots at half-hour intervals and map t_i to the nearest
discrete time point.

756

757

Table 4: Basic statistics of mobility data.

City	Trajectory Point	Temporal Period	User Number	Grid Number
Atlanta	4008w	2016/10/1-2017/9/30	19w	1175
Chicago	17361w	2016/10/1-2017/9/30	33w	1046
Seattle	6184w	2016/10/1-2017/9/30	9.5w	3597
Washington	21415w	2016/10/1-2017/9/30	30w	1361
Los Angeles	35616w	2016/10/1-2017/9/30	65w	4988
New York	30653w	2016/10/1-2017/9/30	94w	6198
Boston	1856w	2016/3/1-2016/3/14	6.2w	1727
Dallas	8000w	2016/3/1-2016/3/14	28w	7936
Miami	1968w	2016/3/1-2016/3/14	7w	924
San Francisco	1744w	2016/3/1-2016/3/14	5.3w	786
Denver	3328w	2016/3/1-2016/3/14	10.6w	5176
Houston	10880w	2016/3/1-2016/3/14	42.4w	16550
Minneapolis	1568w	2016/3/1-2016/3/14	6w	1368
Philadelphia	3168w	2016/3/1-2016/3/14	12w	3525
Phoenix	4912w	2016/3/1-2016/3/14	18w	9475
Portland (OR)	2256w	2016/3/1-2016/3/14	7w	2804

775

776

Table 5: POI categories

finance	café	dormitory
transport	ice cream	shop
health	restaurant	travel agency
education	boutique	office
religion	retail	public transport
food	marketplace	home improvement
fast food	residential	entertainment
shop beauty	recycling	shop transport
commodity	sport	pub
public	livelihood	service
government	accommodation	tourism
kindergarten		

789

790

D EXPERIMENTS DETAILS

791

792

D.1 BASELINES

793

- **Markov** Gambs et al. (2012) The Markov model provides a statistical framework for characterizing how states evolve over time. It predicts future locations by estimating the transition probabilities between states.
- **LSTM** Graves (2012) Long Short-Term Memory networks are highly effective for sequential modeling, as they capture long-term dependencies and temporal dynamics, making them particularly suitable for location prediction tasks.
- **Transformer** Vaswani (2017) The Transformer architecture leverages self-attention mechanisms to process sequential data efficiently, enabling the modeling of long-range dependencies in human mobility patterns.
- **DeepMove** Feng et al. (2018) DeepMove is designed to address the challenges of human mobility prediction by jointly considering spatial, temporal, and personal preference factors that shape individual movement behaviors.
- **GetNext** Yang et al. (2022) GETNext integrates Graph Convolution Networks with Transformers to model global POI transition patterns, incorporating time-aware semantic embeddings for next-location recommendation.

794

795

796

797

798

799

800

801

802

803

804

805

806

807

808

809

Table 6: Popularity rank and value

Popularity Rank	R value
<1%	0
1%-5%	1
5%-10%	2
10%-20%	3
20%-40%	4
40%-60%	5
60%-80%	6
>80%	7

- **CTLE** Lin et al. (2021) The Context- and Time-aware Location Embedding model dynamically generates location embeddings by combining bidirectional Transformers with temporal encoding, capturing multi-faceted semantics of locations under varying spatial-temporal dynamics.
- **Unimove** Han et al. (2025) Unimove is a unified model for multi-city human mobility prediction, employing a trajectory-location dual-tower architecture and MoE Transformer blocks to enhance prediction accuracy across diverse urban environments.
- **TrajGPT** Hsu et al. (2024) TrajGPT is a multitask transformer-based spatiotemporal generative model that frames controlled synthetic trajectory generation as a text infilling problem, ensuring spatiotemporal consistency in visit sequences.
- **TrajFM** Lin et al. (2024) TrajFM is a trajectory foundation model that emphasizes both region transferability and task transferability through its STRFormer backbone.
- **Unitraj** Zhu et al. (2024) UniTraj is a universal trajectory foundation model trained on large-scale, worldwide human mobility data, designed to be both task-adaptive and region-independent.
- **Difftraj** Zhu et al. (2023) DiffTraj is a spatiotemporal diffusion probabilistic model designed for GPS trajectory generation. It employs a Trajectory UNet (Traj-UNet) to reverse a noise process, reconstructing high-fidelity trajectories that preserve the original spatial distributions
- **TrajGAN** Goodfellow et al. (2014) TrajGAN introduces a GAN framework for trajectory generation, where trajectories perturbed with random noise are mapped into realistic sequences by a generator composed of linear and convolutional layers.
- **DiffLSTM** DiffLSTM is a trajectory generation model that integrates the UNet architecture and ResNet blocks from DiffTraj, replacing convolutional layers with Long Short-Term Memory (LSTM) units in the ResNet blocks. This modification allows the model to capture long-range temporal dependencies in sequential data.
- **Movesim** Feng et al. (2020) MoveSim is a generative adversarial network (GAN)-based framework for simulating human mobility patterns. It combines model-based and model-free approaches, utilizing SeqNet for sequential transition modeling and RegNet for incorporating urban structure effects, outperforming existing models in metrics like travel distance and location visits.
- **SAE** Malhotra et al. (2016) SAE is a standard RNN-based sequence-to-sequence architecture trained by minimizing the reconstruction error. The anomaly score for a sequence is determined according to how large its reconstruction error is.
- **GMVSAE** Liu et al. (2020) GMVSAE is a model designed for detecting anomalies in vessel trajectories by employing a Gaussian Mixture Variational Autoencoder, which analyzes historical data and established shipping lanes to identify vessels that deviate significantly from expected paths.

D.2 EXPERIMENT CONFIGURATION

For MoveGPT_{base}, we use a 4-layer Transformer, with a hidden dimension of 512 and 4 attention heads. The pretraining data consists of 6 U.S. cities with a total of 6 million trajectories. For MoveGPT_{ultra}, we employ a 12-layer Transformer with 6 attention heads and a hidden dimension of 768. The pretraining data for includes 16 U.S. cities with a total of 10 million trajectories. All models are trained using the Adam optimizer, with a learning rate of 3×10^{-4} , a maximum of 50 epochs, and early stopping after 3 epochs without improvement. The batch size is set to 32.

D.3 CROSS TASK FINETUNING

Unconditional Generation. We fine-tune MoveGPT on 1,500 specific city trajectories for the tasks of next location prediction and arrival time prediction. After fine-tuning, the model generates a full day’s trajectory by randomly sampling the starting location and time, using a top-k sampling method, and continuing until the predicted time exceeds midnight.

Conditional Generation. We use the embedding of radius of gyration through a linear layer, and add it to the trajectory embedding as the input condition. The rest of the process remains consistent with the unconditional generation.

Table 7: Performance of long term prediction(1 day predict 1 day)

City	Atlanta		Chicago		Seattle		Washington		New York		Los Angeles		Average	
Model	Acc@1	Acc@3												
Transformer	0.109	0.224	0.038	0.074	0.104	0.205	0.073	0.140	0.038	0.072	0.036	0.057	0.066	0.129
DeepMove	0.112	0.243	0.045	0.107	0.115	0.239	0.092	0.200	0.056	0.147	0.055	0.158	0.079	0.182
TrajFM	0.123	0.298	0.093	0.195	0.123	0.279	0.114	0.257	0.086	0.174	0.089	0.182	0.104	0.231
UniTraj	0.131	0.310	0.096	0.201	0.134	0.298	0.121	0.269	0.093	0.217	0.095	0.192	0.112	0.247
MoveGPT_{base}	0.170	0.347	0.127	0.234	0.176	0.349	0.163	0.304	0.126	0.247	0.125	0.221	0.148	0.284
MoveGPT_{ultra}	0.183	0.364	0.142	0.245	0.195	0.359	0.167	0.310	0.143	0.254	0.130	0.223	0.160	0.292

Long-Term Prediction. We use a full-day’s trajectory as the prompt and provide the arrival time for the future trajectory. The model then directly predicts the location corresponding to the given time on the following day.

Anomalous Detection. We take the last token output by MoveGPT and use it through a linear layer to generate the probability output for anomaly detection.

E ADDITIONAL RESULTS

E.1 ABLATION STUDY

SAMoE is the key design of MoveGPT, specifically addressing cross-city data heterogeneity through its specialized gating mechanisms. We conducted systematic ablation studies on five critical configurations: removal of (1) the shared expert, (2) the whole mixture-of-experts, (3) the adapted selector, (4) the temporal router, and (5) the spatial router. Experimental results on Atlanta datasets are shown in Appendix Figure 7. The results demonstrate a consistent performance degradation across all ablated variants. This empirical evidence confirms that each component collectively contributes to effective spatio-temporal pattern modeling, establishing SAMoE’s architectural elements as essential design choices for urban mobility modeling.

E.2 LONG-TERM PREDICTION

Appendix Table 7 shows the result of Long-term prediction.

E.3 CONDITIONAL GENERATION

Appendix Table 8 shows the result of conditional mobility generation.

E.4 ANOMALOUS TRAJECTORY DETECTION

Appendix Table 9 shows the result of anomalous trajectory detection.

E.5 SPATIAL-TIME-ADAPTED ROUTER ANALYSIS

Appendix Figure 8 shows the top-1 percent of features for temporal router during a day in MoveGPT.

E.6 ANALYSIS OF SCALABILITY

Appendix Figure 9 shows the result of scalability performance of MoveGPT.

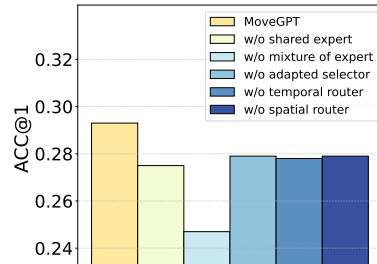


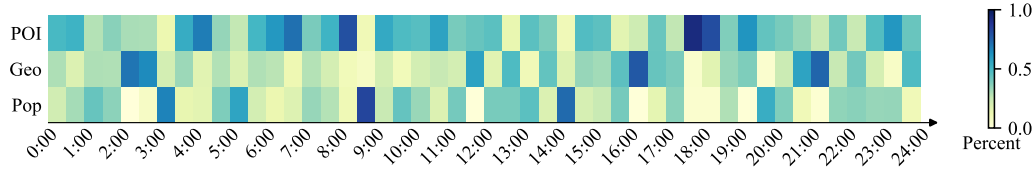
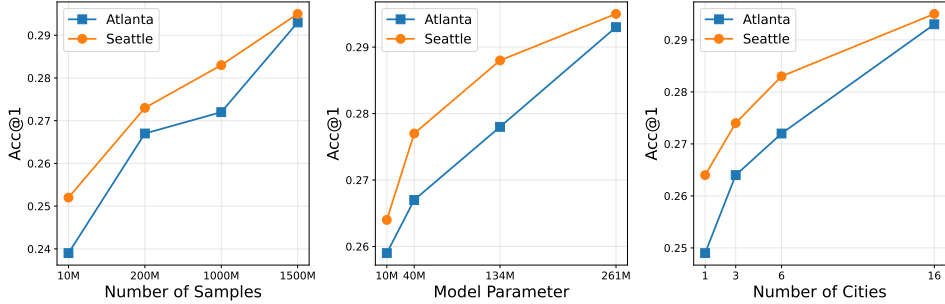
Figure 7: Cross-city transfer performance on Atlanta and Washington dataset.

918
919
920
Table 8: Performance of conditional mobility generation.(Condition: Radius)

921 City	Atlanta		Chicago		Seattle		Washington		New York		Los Angeles		Average	
922 Model	JSD	MAE												
924 Diff-LSTM	0.106	2.511	0.200	3.626	0.035	1.910	0.055	1.962	0.046	5.454	0.048	4.228	0.082	3.282
925 TrajGAN	0.302	7.156	0.731	8.048	0.083	5.750	0.192	4.307	0.169	11.230	0.147	10.186	0.271	7.779
927 MoveSim	0.186	3.848	0.445	3.855	0.036	2.792	0.057	2.095	0.067	5.556	0.084	5.772	0.142	3.986
928 DiffTraj	0.086	1.968	0.155	3.351	0.028	1.804	0.049	1.634	0.022	3.148	0.028	3.689	0.061	2.599
929 Unitraj	0.067	1.803	0.069	3.274	0.042	3.642	0.045	1.667	0.036	4.287	0.086	4.40	0.057	3.185
931 MoveGPT_{base}	0.056	1.792	0.057	2.924	0.028	1.181	0.031	1.275	0.041	2.484	0.041	3.102	0.042	2.126
932 MoveGPT_{ultra}	0.049	1.627	0.042	2.548	0.025	1.074	0.029	1.036	0.033	2.247	0.030	2.866	0.034	1.899

934
935
936
Table 9: Performance of anomalous trajectory detection

937 City	Atlanta		Chicago		Seattle		Washington		New York		Los Angeles		Average	
938 Model	Pre.	Rec.												
939 MLP	0.536	0.586	0.517	0.551	0.541	0.551	0.529	0.634	0.515	0.587	0.506	0.681	0.524	0.598
940 Transformer	0.651	0.629	0.697	0.677	0.705	0.675	0.677	0.623	0.668	0.745	0.718	0.776	0.686	0.687
941 SAE	0.659	0.600	0.701	0.655	0.707	0.651	0.643	0.601	0.630	0.743	0.690	0.748	0.672	0.666
942 GMVSAE	0.763	0.675	0.743	0.745	0.749	0.704	0.715	0.650	0.716	0.822	0.753	0.833	0.740	0.738
943 MoveGPT_{base}	0.840	0.719	0.865	0.787	0.866	0.749	0.836	0.693	0.833	0.892	0.871	0.868	0.852	0.785
944 MoveGPT_{ultra}	0.861	0.733	0.899	0.818	0.891	0.760	0.848	0.699	0.853	0.927	0.879	0.881	0.871	0.803

957
958
959
960
Figure 8: The top-1 percent of temporal router during a day in MoveGPT.961
962
963
964
965
966
967
968
969
970
971
Figure 9: The result of scalability performance of MoveGPT.